MOZ-TIF2-induced acute myeloid leukemia requires the MOZ nucleosome binding motif and TIF2-mediated recruitment of CBP

Kenji Deguchi,[1,7] Paul M. Ayton,[2] Melina Carapeti,[1] Jeffery L. Kutok,[3] Cynthia S. Snyder,[4] Ifor R. Williams,[5] Nicholas C.P. Cross,[6] Christopher K. Glass,[4] Michael L. Cleary,[2] and D. Gary Gilliland[1,7,*]

[1]Division of Hematology and Oncology, Brigham and Women's Hospital and Harvard Medical School, Harvard Institutes of Medicine, 4 Blackfan Circle, Room 420, Boston, Massachusetts 02115
[2]Department of Pathology, Stanford University School of Medicine, 300 Pasteur Drive, Stanford, California 94305
[3]Department of Pathology, Brigham and Women's Hospital, 75 Francis Street, Boston, Massachusetts 02115
[4]Department of Medicine and Cellular and Molecular Medicine, University of California, San Diego, 9500 Gilman Drive, La Jolla, California 92093
[5]Department of Pathology, Emory University School of Medicine, 615 Michael Street, Atlanta, Georgia 30322
[6]Wessex Regional Genetics Laboratory, Salisbury District Hospital, Salisbury, SP2 8BJ, United Kingdom
[7]Howard Hughes Medical Institute, Boston, Massachusetts 02115
*Correspondence: gilliland@calvin.bwh.harvard.edu

Summary

The MOZ-TIF2 fusion is associated with acute myeloid leukemia (AML) with inv(8)(p11q13). MOZ is a MYST family histone acetyltransferase (HAT), whereas TIF2 is a nuclear receptor coactivator that associates with CREB binding protein (CBP). Here we demonstrate that MOZ-TIF2 has transforming properties in vitro and causes AML in a murine bone marrow transplant assay. The C2HC nucleosome recognition motif of MOZ is essential for transformation, whereas MOZ HAT activity is dispensable. However, MOZ-TIF2 interaction with CBP through the TIF2 CBP interaction domain (CID) is essential for transformation. These results indicate that nucleosomal targeting by MOZ and recruitment of CBP by TIF2 are critical requirements for MOZ-TIF2 transformation and indicate that MOZ gain of function contributes to leukemogenesis.

Introduction

Acute myeloid leukemias (AML) are disorders of hematopoietic progenitors characterized by acquired somatic mutations that frequently target transcription factors and transcriptional coactivators. Fusion genes involving transcriptional coactivators that are expressed as a consequence of chromosomal translocations in AML include *MLL/CBP* (Satake et al., 1997; Sobulo et al., 1997; Taki et al., 1997), *MLL/p300* (Ida et al., 1997), *MOZ/CBP* (Borrow et al., 1996), *MOZ/p300* (Chaffanet et al., 2000; Kitabayashi et al., 2001b), *MORF/CBP* (Panagopoulos et al., 2001), and *MOZ-TIF2* (Carapeti et al., 1998; Liang et al., 1998). Each of these fusion proteins contains one or more histone acetyltransferase (HAT) domain(s) that modify chromatin by acetylation of the N-terminal histone tail.

MOZ (monocytic leukemia zinc finger) belongs to the MYST family of histone acetyltransferases and was first cloned as a fusion partner of CBP as a consequence of t(8;16)(p11;p13) associated with the FAB M4/M5 subtype of AML (Borrow et al., 1996). MOZ contains a C4HC3 type PHD zinc finger domain, which may serve as a protein-protein interaction domain (Borrow et al., 1996), an atypical C2HC zinc finger domain with putative nucleosome binding activity, and a region with homology to the active acetyl-coA binding site of several HAT proteins from yeast to *Drosophila* (Chakraborty et al., 2001). The precise function of MOZ is not known, but MOZ displays HAT activity (Champagne et al., 2001; Kitabayashi et al., 2001a), suggesting that it might be involved in the regulation of transcription and chromatin function. Moreover, MOZ possesses a transcriptional repression domain at the N terminus and an activation domain at the C terminus and may thus be involved in both negative and positive regulation of transcription. For example, MOZ regulates transcriptional activation mediated by the hematopoietic transcription factor, Runx1 (AML1) (Kitabayashi et al., 2001a) and a related osteogenic transcriptional factor, Runx2 (Pelletier et al., 2002).

TIF2 is a member of the p160 nuclear receptor transcriptional coactivator family (NRCoAs) (Horwitz et al., 1996; Glass

SIGNIFICANCE

The MOZ-TIF2 fusion is one of several fusion proteins associated with AML that involve transcriptional coactivators, including the MOZ/CBP, MLL/CBP, and MLL/p300 fusions. We demonstrate that transformation by MOZ-TIF2 in vitro and in vivo requires recruitment of CBP through the TIF2 and LXXLL motifs, and thus each of these fusion proteins aberrantly recruits the coactivators CBP or p300. However, in contrast with previous reports that CBP deficiency contributes to pathogenesis of malignancy in humans and in murine models, our data are most consistent with the hypothesis that CBP contributes an oncogenic, rather than tumor-suppressive, function to myeloid transformation by MOZ-TIF2.

et al., 1997) that stimulates gene expression by facilitating the assembly of basal transcription factors into a stable preinitiation complex (Klein-Hitpass et al., 1990). The p160 family, including SRC-1, TIF2/GRIP1, and ACTR/RAC3/pCIP/AIB-1, interacts with nuclear receptors in a ligand-dependent manner and enhances transcriptional activation by the receptor via histone acetylation/methylation (Leo and Chen, 2000).

The p160 family of coactivators have a common domain structure, with a conserved N-terminal bHLH-PAS domain, a centrally located receptor interaction domain (RID), and a C-terminal transcriptional activation domain (AD). The RID contains three conserved motifs, LXXLL (where L is leucine and X is any amino acid), that are required to mediate interactions between coactivators and liganded nuclear receptors (Heery et al., 1997; Torchia et al., 1997; Ding et al., 1998). TIF2, as well as SRC-1 or pCIP, interacts directly with CBP via three conserved imperfect LXXLL motifs in the CBP interaction domain (Torchia et al., 1997; Demarest et al., 2002).

The MOZ-TIF2 fusion protein retains the C4HC3 type PHD zinc finger domain, and the HAT (MYST) domain of MOZ. The TIF2 moiety in MOZ-TIF2 retains the CBP interaction domain (CID) and CBP-independent activation domain (called AD2) of TIF2 (Figure 1A). MOZ-TIF2 lacks the C terminus of MOZ and the PAS/bHLH DNA binding/protein heterodimerization domain and nuclear receptor interaction domain of TIF2.

We demonstrate here the transforming properties of MOZ-TIF2 in primary murine hematopoietic progenitors in vitro and in vivo. Mutational analysis was performed to determine the role of the various functional domains retained in the MOZ-TIF2 fusion. Our data are consistent with the hypothesis that MOZ-TIF2 results in MOZ gain of function through recruitment of CBP to the nucleosome by the MOZ C2HC domain and suggest the novel finding that CBP contributes an oncogenic, rather than tumor-suppressive, function to myeloid transformation by MOZ-TIF2.

Results

MOZ-TIF2 immortalizes primitive myeloid progenitors, and immortalization is dependent on the MOZ MYST domain and the TIF2 CID

The transforming properties of MOZ-TIF2 and related mutants were studied in vitro by retroviral transduction of murine bone marrow cells in a serial replating assay (Lavau et al., 1997, 2000a, 2000b; Slany et al., 1998; DiMartino et al., 2000). MOZ-TIF2 mutants included deletions of the PHD domain of (del PHD/TIF2), the MOZ HAT domain (del HAT/TIF2), the TIF2/CBP interaction domain (MOZ/del CID) and a fusion in which only the TIF2 CBP interaction domain was present (MOZ/CID) (Figure 1B). We confirmed the protein expression of MOZ-TIF2 or mutants in 293T cells transiently transfected with flag-tagged *MSCV* constructs by Western blotting (Figure 1C).

Bone marrow cells transduced with MOZ-TIF2 or deletion mutants were plated in methylcellulose cultures supplemented with SCF, IL-3, and IL-6. G418 was also added to first round cultures to select for transduced cells. In the first round of plating, numerous colonies were observed for cells transduced with *MOZ-TIF2* or related deletion mutants as well as empty vector, reflecting the normal clonogenic potential of progenitors harvested from 5-FU-treated bone marrow. Fewer first round colonies were observed with *MOZ-TIF2* or deletion mutants than

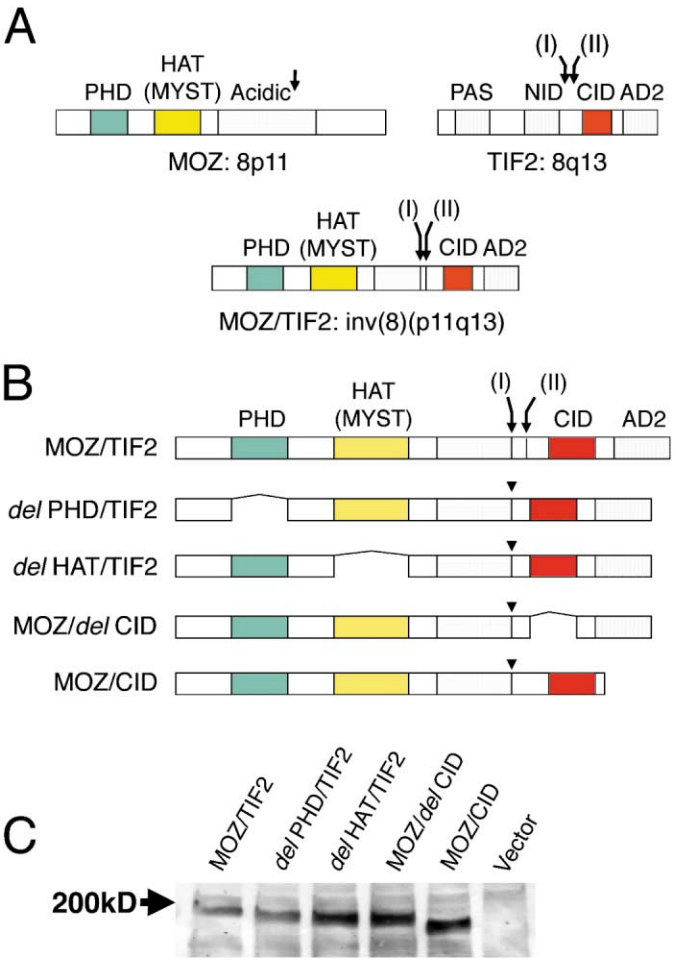

Figure 1. Schematic diagram and Western blot analysis of MOZ, TIF2, MOZ-TIF2 fusion, and MOZ-TIF2 deletion mutants

A: Two variants of MOZ-TIF2 have been reported in the literature. Arrow indicates the breakpoint region in the inv(8). Domains for MOZ are as follows: PHD, plant homeodomain zinc fingers; HAT, histone acetyltransferase or MYST, [MOZ, YBF2/SAS3, SAS2, TIP60]. Domains for TIF2 are: CID, CBP interaction domain; and RID, nuclear receptor interaction domain; PAS/bHLH, DNA binding/protein heterodimerization domain; AD2, activation domain 2.
B: The fusion retains the PHD domain and the HAT domain of MOZ and the CID and the AD2 domains of TIF2.
C: Western blot analysis of MOZ-TIF2 and related deletion mutants expressed from the *MSCV* constructs in transiently transfected 293T cells using anti-M2 Flag antibody.

empty vector controls (Figure 2A, first round). This is probably due to lower viral titers of MOZ-TIF2 constructs compared with empty vector, as a consequence of inefficient viral packaging of the large MOZ-TIF2 constructs.

First round colonies were harvested, and 10^4 cells were plated in secondary methylcellulose cultures. In second round cultures, *MOZ-TIF2*-transduced cells produced hundreds of large, compact colonies with primitive GM morphology. Among the various deletion mutants, *del PHD/TIF2* and *MOZ/CID* generated secondary colonies, whereas cells transduced with *del HAT/TIF2*, *MOZ/del CID*, or empty vector control produced no colonies (Figure 2A, second round). This effect was sustained through a subsequent third round of plating (Figure 2A, third round). These data indicate that the MOZ HAT and TIF2 CID

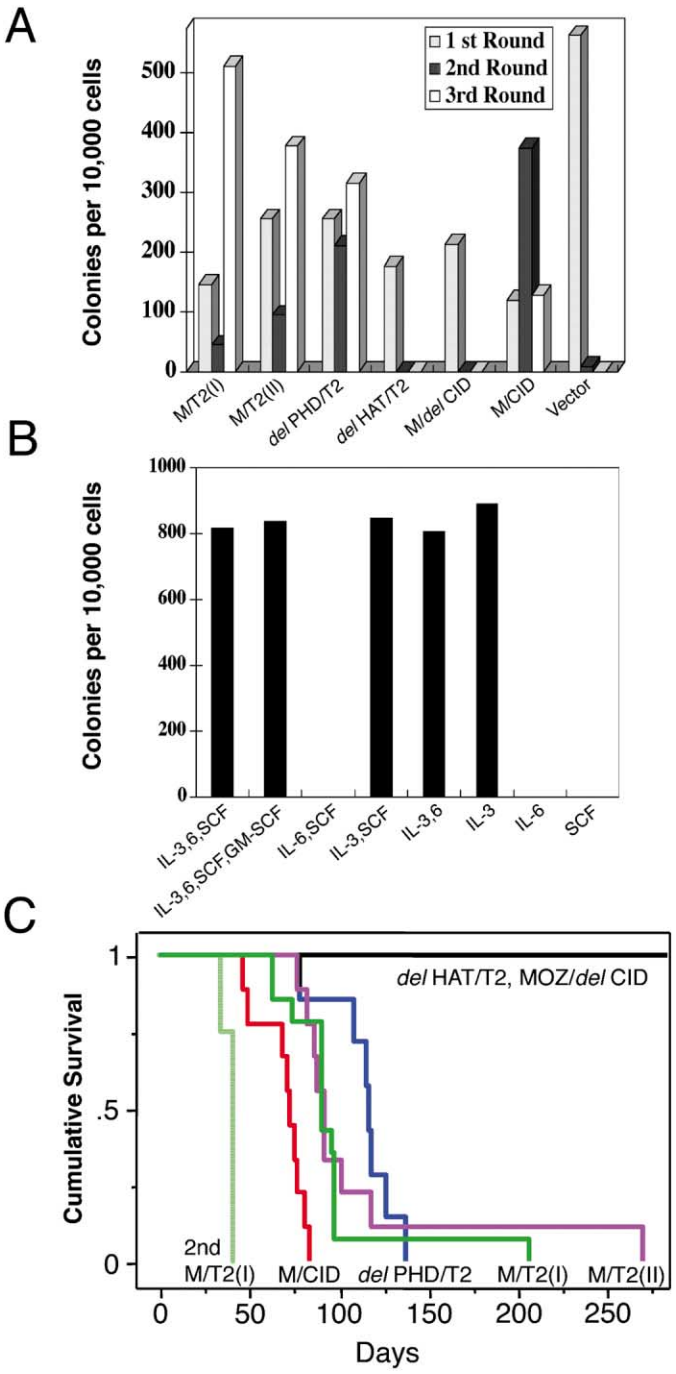

Figure 2. Transforming activity of MOZ-TIF2 and related mutants in serial replating and BMT assays

A: Number of first, secondary, and tertiary colonies (from left to right) generated per 10^4 input cells seeded following methylcellulose culture of bone marrow cells transduced with the MOZ-TIF2 or deletion mutants. The values shown are the mean of two independent experiments with duplicate.

B: Number of colonies generated from MOZ-TIF2 third round platings with various combinations of cytokines.

C: Kaplan-Meier comparative survival analysis of MOZ-TIF2 and deletion mutants. BMT cumulative survival was plotted against days posttransplantation. Mice transplanted with primary murine bone marrow transduced with MOZ-TIF2(I) (n = 14), MOZ-TIF2(II) (n = 9), del PHD/TIF2 (n = 7), or MOZ/CID (n = 9) developed AML with a median latency of 91, 92, 117 or 73 days, respectively. A secondary BMT (n = 4) using 1×10^6 cells from the cervical node of MOZ-TIF2(I) diseased mice caused AML rapidly with a median latency of 40 days. In contrast, mice transplanted with bone marrow retrovirally transduced with del HAT/TIF2 or MOZ/del CID developed no disease with an observation period of more than 300 days. Eight control mice transplanted with bone marrow transduced by retrovirus containing either the wild-type MOZ or TIF2 were alive and well up to 280 days posttransplantation (not shown).

domains are required for in vitro transformation, whereas the MOZ PHD domain and the putative acetyltransferase domain (AD2) of TIF2 are not required for transformation.

We also tested the myeloid immortalization capacity of MOZ-TIF2 with a growth factor cocktail including macrophage colony-stimulating factor (GM-CSF). MOZ-TIF2 was unable to immortalize myeloid progenitors under these conditions (data not shown).

To determine whether MOZ-TIF2-transduced cells were capable of sustained growth in suspension cultures, colonies from MOZ-TIF2 third round platings were replated for one additional round with various combinations of cytokines. Each culture was initiated with 10^4 cells. As shown in Figure 1B, MOZ-TIF2-transduced cells produced almost the same number of myeloid colonies with IL-3 alone or the growth factor cocktail including IL-3. In contrast, no colonies were observed without IL-3 (Figure 2B). These data indicate that cells immortalized by MOZ-TIF2 require exogenous IL-3 for sustained viability or growth.

MOZ-TIF2 induces acute myeloid leukemia in a murine bone marrow transplant assay

To assess in vivo transforming properties of MOZ-TIF2, we performed murine bone marrow transplant assays as described (Schwaller et al., 1998; Liu et al., 2000). Briefly, whole bone marrow harvested from 5-fluorouracil-primed mice was transduced with retrovirus containing the *MOZ-TIF2* fusion gene. The retroviral vector contained a cassette with an internal ribosomal entry site (IRES) and EGFP. *MOZ-TIF2*-transduced bone marrow cells were introduced by tail vein injection into lethally irradiated syngeneic recipient mice. In control experiments, mice transplanted with bone marrow cells transduced with retrovirus containing either MOZ or TIF2 wild-type genes did not develop hematological disease with a followup of more than 280 days (data not shown).

In contrast, animals transduced with cells containing either the *MOZ-TIF2(I)* or *MOZ-TIF2(II)* variant fusion genes developed fatal hematopoietic malignant disease with a median latency of 93 days or 90 days, respectively. The disease was readily transplantable into secondary recipients with a shorter disease latency of 35–42 days (Figure 2C and Table 1). Gross pathological analysis revealed generalized lymphadenopathy, including axillary, mesenteric, paraaortic, and femoral nodes in all diseased mice. In addition, all mice had widespread infiltration of tumor within the cervical nodes and salivary glands, spreading in some cases and involving the entire cranio/facial region. Additional features of malignancy included splenomegaly (150 mg–500 mg) and hepatomegaly (Table 1). We consistently observed elevated white blood cell (WBC) counts that ranged from 30×10^6/ml to as high as 220×10^6/ml (Table 1). These cells were predominantly comprised of mature myeloid and monocytic forms, including admixed immature myeloid elements, many with monocytic features, and occasional leukemic blast forms (Figure 3A-a). The majority of cells observed in lymph node

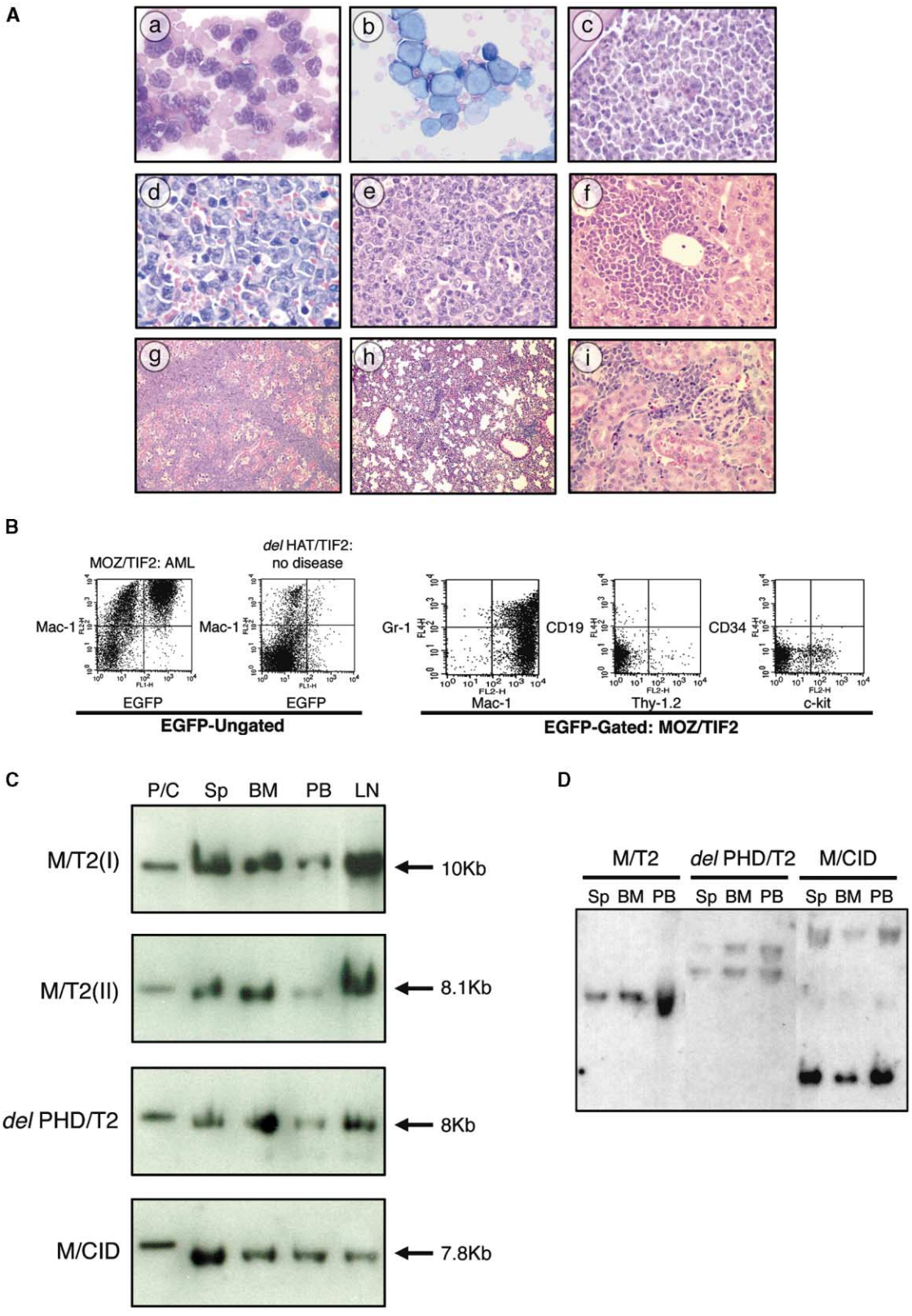

Figure 3. Histopathologic, flow cytometric, and clonality analysis of mice transplanted with MOZ-TIF2-transduced bone marrow

A: (a) Peripheral blood smears (Wright-Giemsa stain) showed a moderate leukocytosis consisting predominantly of mature and immature myeloid cells, many with monocytic features and occasional blast forms. **(b)** A touch preparation of cervical lymph node (Wright-Giemsa stain) showed large immature myeloid forms with high nuclear to cytoplasmic ratios. **(c)** Representative bone marrow from an affected mouse showed that the majority of the cellularity was comprised of sheets of immature myeloid cells with oval to irregular nuclei, 1–3 distinct nucleoli, and small to moderate amounts of eosinophilic cytoplasm. Also present were smaller numbers of mature myeloid cells. The features were consistent with involvement by a myeloid leukemia. **(d)** Spleens

Table 1. Summary of bone marrow transplant experiments with MOZ-TIF2 and deletion mutants

Construct	No. of diseased mice/BMT mice	Disease latency (median)	WBC $\times$ 10^6 per ml (median)	Spleen weight, mg (median)
MOZ-TIF2(I)	14/14	36–207 (91)	30–220 (71)	170–540 (388)
MOZ-TIF2(II)	9/9	77–270 (92)	17.5–159 (57)	260–390 (300)
del PHD/TIF2	7/7	78–138 (117)	27–215 (92)	210–590 (510)
MOZ/CID	9/9	47–84 (73)	59–254 (115)	120–570 (310)
2nd BMT (MOZ/TIF2(I))	4/4	35–42 (42)	70–92 (80)	250–715 (525)
del HAT/TIF2	0/8	No disease >300 days		
MOZ/*del* CID	0/8	No disease >300 days		

Note: Normal WBC count is up to 15 $\times$ 10^6 per ml and normal spleen weight is up to 150 mg.

touch preparations were immature myeloid cells including large immature myeloid forms with high nuclear to cytoplasmic ratios (Figure 3A-b).

Histological examination of tissues from diseased animals demonstrated systemic involvement by a similar population of myeloid leukemia cells. Bone marrow (Figure 3A-c) revealed sheets of immature myeloid cells with oval to irregular nuclei, 1–3 distinct nucleoli, and small to moderate amounts of eosinophilic cytoplasm. Also present were smaller numbers of maturing myeloid cells. All spleens from representative diseased mice had marked expansion of the red pulp by extramedullary hematopoiesis composed predominantly of sheets of myeloid elements demonstrating a limited degree of maturation and fewer numbers of erythroid islands and megakaryocytes (Figure 3A-d). Mesenteric lymph nodes from representative mice showed marked lymphoid depletion and diffuse effacement of the nodal architecture by a homogeneous population of immature myeloid cells with varying degrees of differentiation (Figure 3A-e). In addition, the liver revealed a predominantly periportal, perivascular, and sinusoidal mononuclear infiltrate, comprised predominantly of immature myeloid forms similar to the bone marrow and splenic infiltrates (Figure 3A-f). Of note, salivary glands (Figure 3A-g) in most of the animals had infiltrates morphologically identical to those seen in the liver, spleen, lymph nodes, and marrow, with extensive salivary gland destruction in the majority of cases. The lungs showed an interstitial infiltrate of immature and maturing myeloid forms (Figure 3A-h), and the kidneys in the majority of animals had scattered perivascular myeloid infiltrates (Figure 3A-i).

Flow cytometric analysis for lineage-specific antigens and EGFP on single cell suspensions from the spleen of diseased animals transplanted with MOZ-TIF2 demonstrated that 30%–60% of cells in the spleen were positive for EGFP (Figure 3B, Ungated). When gated for EGFP, the vast majority of cells were positive for Mac-1, confirming the myeloid lineage of these cells. A fraction of Mac-1-positive cells (40%) also expressed the mature granulocytic marker Gr-1 (Figure 3B, EGFP-Gated) although at lower levels than observed on mature granulocytes. The mature monocyte- or macrophage-specific marker, F4/80, was not detected on these cells (data not shown). None of the EGFP-gated populations infiltrating affected tissues expressed B (CD19) or T (Thy-1.2) lymphocyte markers (Figure 3B, EGFP-Gated). There was no CD34 expression on these cells and low levels of expression of c-kit, a marker associated with primitive hematopoietic cells (Figure 3B, EGFP-Gated). These results indicate that the cells infiltrating the affected tissues are relatively immature myeloid cells with partial granulocytic differentiation.

The MOZ MYST domain and the TIF2 CBP interaction domain are essential for leukemogenesis

Deletion mutants of *MOZ-TIF2* were next tested in the murine BMT model. Functional domains required for MOZ-TIF2 leukemogenesis correlated with the results from the serial replating assay. The *del PHD/TIF2* or *MOZ/CID* mutants caused fatal hematologic malignancy in all animals with a median latency of 113 days or 73 days, respectively (Figure 2C and Table 1). In contrast, deletion mutants lacking the MOZ MYST domain or the TIF2 CID did not cause hematological disease within an observation period of 330 days (Figure 2C and Table 1). Histopathological and flow cytometric analyses showed that the dis-

from representative MOZ-TIF2 animals showed expansion of red pulp by sheets of immature and maturing myeloid forms. **(e)** A mesenteric lymph node mass from a representative mouse showed marked lymphoid depletion and diffuse effacement of the nodal architecture by a homogeneous population of immature myeloid cells with varying degrees of differentiation. **(f)** Livers from representative diseased animals showed extensive perivenular and sinusoidal mononuclear infiltrates, comprised predominantly of immature myeloid forms similar to the bone marrow and splenic infiltrates. **(g)** Salivary glands in some diseased animals demonstrated infiltrates morphologically identical to those seen in the liver, spleen, lymph nodes, and marrow. Extensive salivary gland destruction was present in the majority of cases. **(h)** Lungs demonstrated an interstitial infiltrate of immature and maturing myeloid forms. **(i)** Kidneys in the majority of animals demonstrated scattered perivascular myeloid infiltrates.

B: Flow cytometric analysis of spleens following transplantation of mice with bone marrow transduced with MOZ-TIF2 or delHAT/TIF2. Spleen cells were stained with a combination of antibodies to Mac-1 and Gr-1, Thy1.2 and CD19, or c-kit and CD34. Dot plots of cell gated on scatter profile only (Ungated) or scatter profile and EGFP expression (EGFP Gated) are shown in left panels and right panels, respectively. Splenic cells show a predominant population of EGFP-positive cells that expresses myeloid markers (Mac-1 and/or Gr-1) and lacks staining for B cell (CD19) and T cell (Thy-1.2) markers. A few of these cells also express c-kit. A major subset of these cells in the spleen demonstrates strong Mac-1 staining with low to absent amounts of Gr-1, indicating that the leukemic cells were relatively immature myeloid cells with partial granulocytic differentiation.

C and **D:** Proviral integration and clonality of mice with bone marrow transduced with MOZ-TIF2. Southern blot analysis of DNA isolated from various tissues of primary recipients with various *MSCV-EGFP* constructs. Sp, spleen; BM, bone marrow; PB, peripheral blood; LN, lymph node. NheI cuts in the viral LTR producing a band of expected size in tissues that contain provirus. EcoRI cuts once in the provirus, resulting in bands of different sizes corresponding to different genomic integration sites. One discrete band can be seen indicating the clonal nature of disease in these tissues.

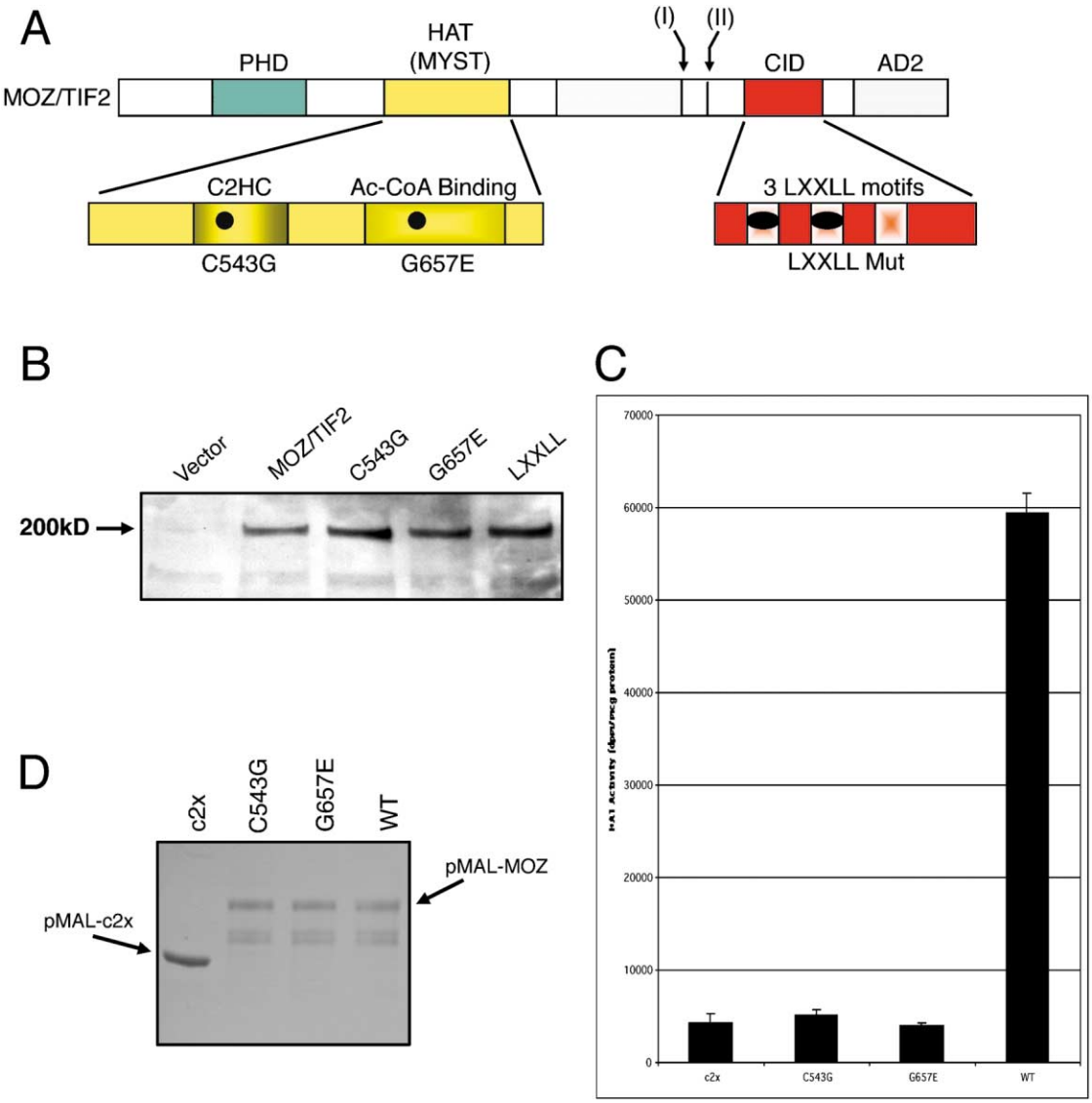

Figure 4. Structure and enzymic activity of MOZ-TIF2 point mutants

A: Schematic diagram of mutations. Conserved amino acids C of C2HC zing finger or G of Ac-CoA binding motif in HAT domain were replaced with G (MOZ-TIF2 C543G) or E (MOZ-TIF2 G657E), respectively. The MOZ-TIF2 LXXLL mutant was generated by replacing amino acid residues in the first two LXXLL motifs (PDDLL→PAAAA and LLDQL→AADGA) in the CID.

B: Transient transfection followed by Western blot analysis of FLAG-tagged mutants demonstrated expression of the appropriate size protein for each mutant.

C: MOZ HAT activity is abrogated in the C543G or G657E mutants. Bacterially expressed fusion proteins of the *E. coli* maltose binding protein (MBP) and segments of human MOZ were affinity purified and tested for histone acetyltransferase (HAT) activity using filter binding assays. Incorporation of tritiated acetyl coenzyme A into free calf thymus histones was catalyzed by affinity-purified MBP-MOZ wild-type or mutant fusion proteins. The MYST domain of MOZ demonstrated histone acetyltransferase activity (pMAL-MOZ-WT). Fusions encoding a point mutation within the C2HC zinc finger (C543G) or a point mutation within the acetyl coenzyme A binding motif (G657E) demonstrated abrogation of HAT activity. The maltose binding protein tag present in the empty vector (c2x) did not demonstrate HAT activity.

D: Gel analysis of 2 μg of affinity-purified MBP and MBP-MOZ proteins used in HAT assays.

ease caused by the *del PHD/TIF2* or *MOZ/CID* constructs was AML, indistinguishable from disease induced by full-length MOZ-TIF2 (Table 1).

To verify the presence of the *MOZ-TIF2* and related mutant proviruses in the affected tissues, Southern blot analyses were performed on genomic DNA isolated from various tissues using an EGFP probe. Genomic DNA was digested with NheI, which cleaves in each of the flanking LTRs within the retrovirus. We identified intact proviral integration as a single band of the expected size in spleen, bone marrow, peripheral blood, and mesenteric lymph node from animals transplanted with bone marrow cells transduced with *MOZ-TIF2*, *del PHD/TIF2*, or *MOZ/CID*, reflecting the pattern of widespread disease seen on histopathological examination (Figure 3C).

Clonality of tumors was assessed using EcoRI, which cleaves once in the integrated provirus. We typically observed

distinct 1-2 integration sites in various tissues analyzed (Figure 3D), indicating that the tumors were monoclonal or biclonal in nature. These data suggest that secondary mutations may be required for the development of the AML phenotype.

The MOZ C2HC nucleosome binding motif is essential for transformation, whereas acetyltransferase activity is dispensable

In vitro and in vivo structure-function analysis showed that the MOZ HAT domain was essential for MOZ-TIF2-mediated transformation. Like other MYST family members, the MOZ HAT domain contains both a C2HC zinc finger nucleosome binding motif and an acetyl transferase catalytic domain that binds to acetyl-Co-enzyme A (Ac-CoA) (Figure 4A) (Sterner and Berger, 2000). Mutational analyses of the yeast and *Drosophila* homologs of MOZ (Sas3 and Mof, respectively) have shown that both the C2HC zinc finger domain and Ac-CoA binding domain are required for HAT activity (Takechi and Nakayama, 1999; Akhtar and Becker, 2000). Moreover, the Mof C2HC zinc finger motif is required for binding to the nucleosome (Akhtar and Becker, 2001).

To determine the relative contributions of these functional motifs within the MOZ MYST domain, we generated point mutations in *MOZ-TIF2* at amino acid residues C543G and G657E, respectively (Figure 4A). These are homologous to mutations that abrogate C2HC nucleosome binding or acetyltransferase activity, respectively, in the context of the MOZ homologs Sas3 and Mof (Takechi and Nakayama, 1999; Akhtar and Becker, 2000, 2001).

We confirmed predicted functional effects of these mutations by expressing the MYST domain of MOZ with the point mutation in the C2HC zinc finger domain (C543G) or the Ac-CoA binding site (G657E) in *E. coli*. HAT activity was determined by measuring the incorporation of [^{3}H]acetyl CoA into calf thymus histones in liquid assays. HAT activity of MOZ was completely abrogated by either the C543G mutant or the G657E mutant, a finding that is consistent with a requirement for the conserved MOZ C2HC zinc finger motif and the Ac-CoA binding motif for binding to and acetylation of histones, respectively (Figures 4C and 4D).

The mutants were next tested in the serial replating and murine BMT assays. In both assays, the C543G mutation resulted in complete loss of transformation, indicating that nucleosome binding motif was essential. In contrast, the G657E Ac-CoA binding mutant retained transforming ability in both assays, indicating that MOZ acetyltransferase activity was dispensable (Figures 5A and 5B). Although penetrance of AML was reduced to 50%, the latency was identical to MOZ-TIF2. One animal transplanted with the G657E mutant developed a T cell malignancy (data not shown), but the others developed AML that was indistinguishable from the MOZ-TIF2 phenotype by histopathology or flow cytometry. Thus, the Ac-CoA binding motif is dispensable for development of AML, but its absence may affect the penetrance and, in some instances, phenotype of disease.

Recruitment of CBP by MOZ-TIF2 is required for transformation

TIF2 activity is stimulated through interaction with CBP via the CBP interaction domain (CID) (Voegel et al., 1998). We hypothesized that the recruitment of CBP by TIF2 CID contributed to leukemogenesis by MOZ-TIF2 because the MOZ-TIF2 mutant lacking the TIF2 CID abrogated transformation in vitro and in vivo. In contrast, a mutant in which MOZ was fused to only the TIF2 CID domain, and lacking the TIF2 AD2 carboxy-terminal domain, retained full transforming properties.

To verify this hypothesis, we tested for CID-mediated association of MOZ-TIF2 with CBP using GST pulldown assays. A GST-CBP (murine CBP amino acids 2040–2200, containing the p160 interaction domain of CBP) fusion protein expressed in *E. coli* was used for experiments with in vitro translated MOZ-TIF2 and related mutants. MOZ-TIF2, del PHD/TIF2, del HAT/TIF2, and MOZ/CID all associated with GST-CBP (Figure 6). In contrast, only MOZ/del CID did not bind to GST-CBP, indicating that MOZ-TIF2 associates with CBP through the TIF2 CID.

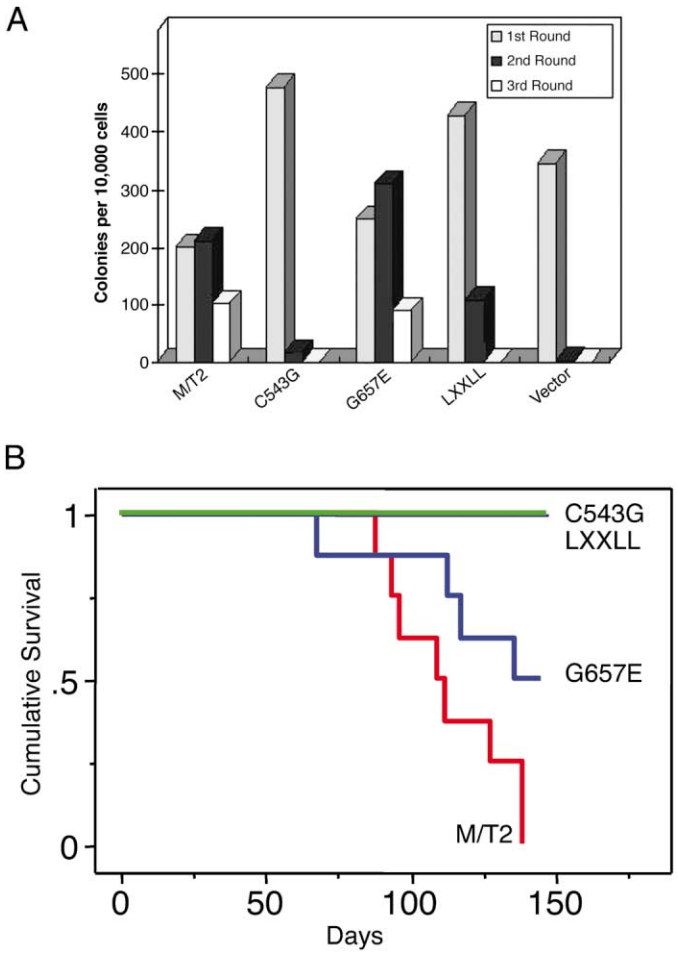

Figure 5. Myeloid immortalization assays and Kaplan-Meier comparative survival analysis of MOZ-TIF2 point mutants

A: Numbers of primary, secondary, and tertiary colonies (from left to right) generated per 10^4 input cells transduced with MOZ-TIF2 and related mutants. The values shown are the mean to two independent experiments with duplicate values.

B: Kaplan-Meier plot of survival. Over 150 days, mice transplanted with primary bone marrow cells transduced with MOZ-TIF2 (n = 8) or MOZ-TIF2 G657E (n = 8) developed hematologic disease with an 88% penetrance (all AML) or 50% penetrance (three AML and one T cell lymphoma), respectively. In constrast, mice transplanted with bone marrow retrovirally transduced with MOZ-TIF2 C543G (n = 9) or LXXLL (n = 8) mutations developed no disease.

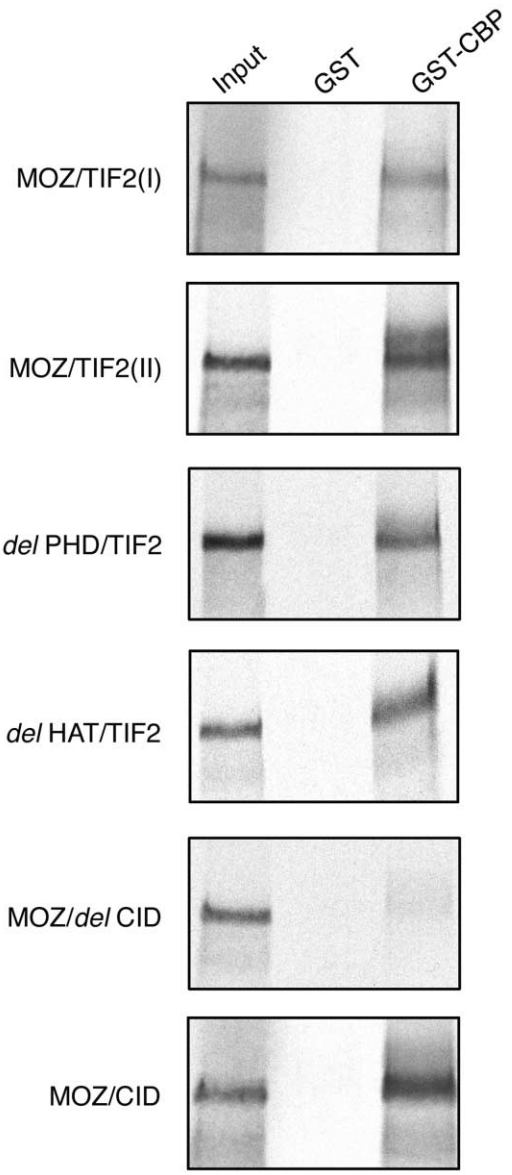

Figure 6. MOZ-TIF2 interacts with CBP

In vitro translated and 35S-labeled MOZ-TIF2 or related deletion mutants were incubated with beads absorbed with GST (lane 2) or GST-CBP (murine CBP aa2040–2200) (lane 3). Labeled peptides retained on the beads were released and analyzed by SDS-PAGE and autoradiography, together with 15% of the translated products used in the incubation (INPUT, lane 1).

We tested the transforming properties of *MOZ-TIF2* with loss-of-function point mutations in the LXXLL motif that is required for CBP interaction (Voegel et al., 1998). The first two LXXLL motifs (PDDLL→PAAAA and LLDQL→AADGA) in the CID were mutated (Figure 4A). In the serial replating assay, this mutant (*MOZ-TIF2 LXXLL*) did not generate any colonies in second and third round replatings, indicating that the LXXLL mutations in the TIF2 CID abolished the immortalization properties of MOZ-TIF2 in this assay (Figure 5A).We next tested the transforming properties of the MOZ-TIF2 LXXLL mutants in vivo. None of eight animals transplanted with bone marrow retrovirally transduced with *MOZ-TIF2 LXXLL* developed hematological disease (Figure 5B). These data indicate that the conserved LXXLL motifs in the TIF2 CID that are required for CBP interaction are necessary for in vitro and in vivo transformation mediated by MOZ-TIF2. Collectively, these findings demonstrate that the association between MOZ-TIF2 and CBP through the TIF2 CID plays a pivotal role in MOZ-TIF2-mediated transformation (Figure 7).

Discussion

In this study, we demonstrate that MOZ-TIF2 immortalizes myeloid progenitors in vitro and induces AML in mice. The murine disease shares many features with human leukemias that express MOZ-TIF2 as a consequence of inv(8)(p11q13). Our successful modeling of this leukemia in mice reveals several important aspects of its pathogenesis and demonstrates the in vivo myeloid transforming properties of MOZ-related fusion proteins, which also include MOZ/CBP and MOZ/p300.

Our studies suggest that MOZ-TIF2 specifically cooperates with the IL-3 signaling pathway to facilitate immortalization since IL-3 was found to be necessary and sufficient for maintenance of in vitro clonogenic activity of myeloid progenitors transduced with MOZ-TIF2. Conversely, GM-CSF appeared to antagonize immortalization, suggesting that signaling via the GM-CSF receptor pathway in primary target cells induces terminal differentiation independent of MOZ-TIF2 expression and/or the presence of other cytokines such as IL-3. However, after establishment of MOZ-TIF2-immmortalized myeloid progenitors in vitro, GM-CSF was unable to overcome IL-3-mediated clonogenic activity, suggesting that MOZ-TIF2-immortalized cells become nonresponsive to GM-CSF. Thus, MOZ-TIF2-immortalized cells are phenotypically distinct from the initial target populations from which they are derived. Attenuation of GM-CSF-mediated terminal differentiation may be due to receptor downregulation or functional loss of essential downstream signaling components. This contrasts with the effects of various MLL fusion proteins, which immortalize myeloid progenitors in vitro in the presence of multiple cytokines including GM-CSF (reviewed in Ayton and Cleary, 2001) and are thought to act via abrogation of both IL-3- and GM-CSF-mediated terminal differentiation.

Animals transplanted with MOZ-TIF2-transduced cells developed AML with 100% penetrance with a relatively short latency. The phenotype of these animals was similar in many ways to the AML phenotype associated with inv(8) in humans, including a predominance of myeloid cells with features of immature monocytes. AML was readily transplantable to secondary recipients, suggesting that the disease may arise from stem cells or immature progenitors with self-renewal capacity. The mono- or oligo-clonality of the disease as well as the defined latency indicate that secondary mutations are required for progression to a fully malignant AML phenotype. The nature of potential secondary mutations is suggested by the recent report that an AML with inv(8) also contained an internal tandem duplication (ITD) of the FLT-3 receptor (Billio et al., 2002). FLT-3 ITD results in constitutively activated tyrosine kinase activity that is sufficient to induce myeloproliferative disease (but not AML) in a murine bone marrow transplant model (Kelly et al., 2002). Thus, constitutive activation of the FLT-3 pathway may represent a candidate secondary mutation that cooperates with MOZ-TIF2 to abrogate factor dependence and induce AML.

Mutational analysis of MOZ-TIF2 suggests a mechanistic

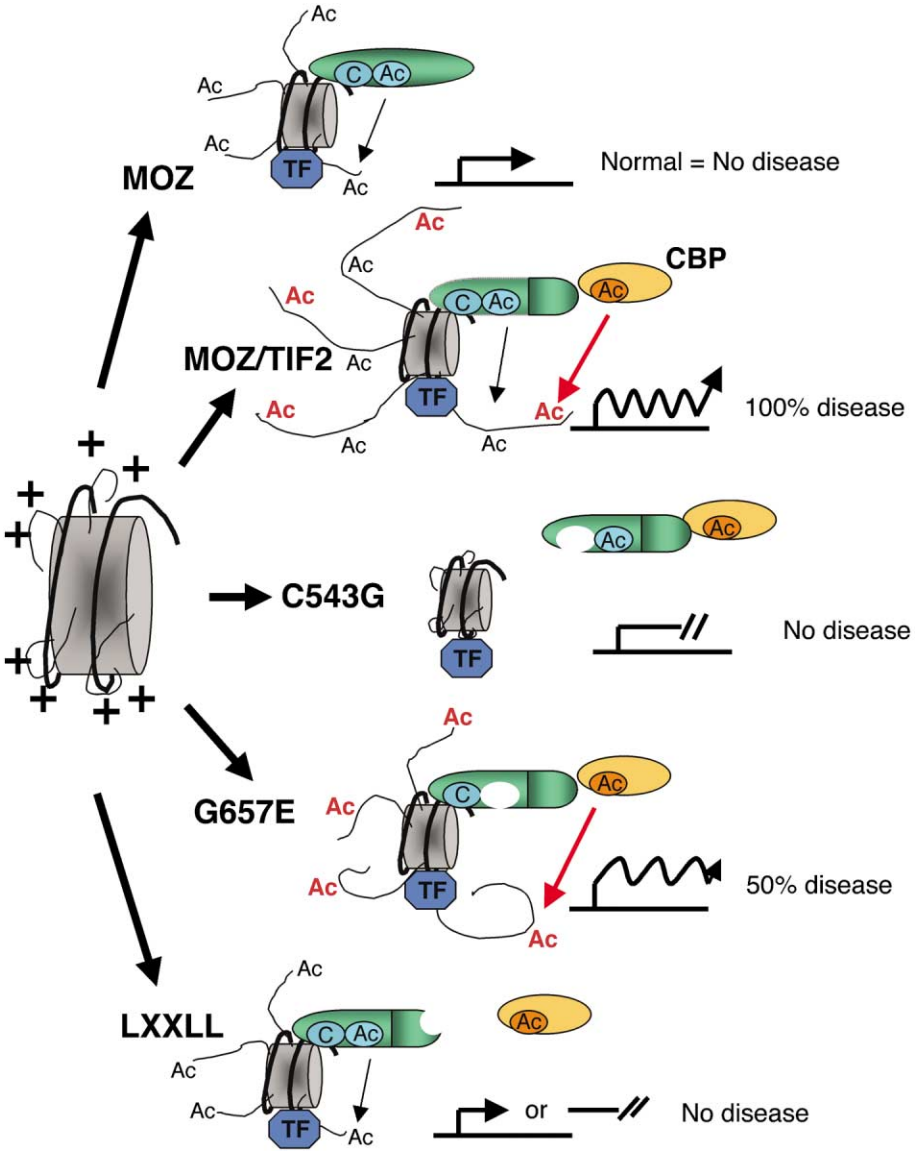

Figure 7. Model for transformation mediated by the MOZ-TIF2 fusion protein

Wild-type MOZ binds to nucleosomes via the C2HC domain and mediates acetylation of histones through HAT activity in the MYST domain. The MOZ-TIF2 fusion recruits CBP to the nucleosome and results in aberrant acetylation of histones, and perhaps of critical associated transcription factors, resulting in leukemia with complete penetrance. Mutation C543G abrogates nucleosome binding activity of MOZ-TIF2 and results in abrogation of leukemia in that neither the MOZ MYST domain nor the CBP HAT activity recruited through the TIF2 CBP interaction domain are targeted to nucleosomes. The MOZ G657E mutation that abrogates MOZ HAT activity attenuates but does not eradicate transforming activity in that CBP HAT activity can still be recruited to the nucleosome via the MOZ-TIF2 fusion. Finally, mutation of the TIF2 LXXLL motif required for CBP interaction results in abrogation of leukemia due to a lack of CBP recruitment. Collectively, these data suggest that MOZ-TIF2-induced leukemias require recruitment of CBP to MOZ nucleosome binding sites, and are the consequence of a MOZ gain-of-function mutation. Further, the model suggests that CBP can act as an oncogene. Abbreviations: Ac = acetylation site; C = MOZ C2HC nucleosome binding domain; TF = transcription factor. Green indicates MOZ and related mutants, yellow indicates CBP. Ac within the MOZ and CBP proteins indicates acetyl-CoA transferase domain.

basis for its oncogenic function. The PHD zinc finger domain at the N terminus of MOZ is dispensable for transformation, indicating that transcriptional repression previously associated with this domain (Champagne et al., 2001) is not required for transformation by MOZ-TIF2. Moreover, loss of the C terminus of MOZ as a consequence of chromosomal translocation is not sufficient for leukemogenesis since a mutant lacking the TIF2 moiety is not transforming. In contrast, deletion of the MOZ HAT domain abrogated MOZ-TIF2-mediated transformation. The HAT (or MYST) domains of MYST family proteins contain two tandem motifs that are highly conserved from yeast to mammals. The first conserved motif is an atypical C2HC zinc finger motif, which in the MOZ-related protein Mof, has been demonstrated to be a nucleosome recognition domain (Akhtar and Becker, 2001). The second motif encodes an acetylcoenzyme A (acetyl CoA) binding domain (also seen in other HATs), which transfers the acetyl moiety from acetyl CoA onto one or more lysine residues contained within the N-terminal tails of histones (Grant and Berger, 1999). The relative contributions of these two subdomains of MOZ-TIF2 were evaluated following their functional inactivation by point mutations. The C543G mutation is precisely analogous to a mutation that abrogates nucleosome recognition and binding of the *Drosophila* ortholog of MOZ, Mof. The observation that either the C543G or the G567E mutation abrogates HAT activity in MOZ is consistent with a conserved function for these residues in MOZ and Mof, but would be further strengthened by direct demonstration that C543G results in loss of nucleosome binding in vitro. Taken together, however, these data are consistent with the hypothesis that target recognition, rather than MOZ-mediated acetylation, is a critical contribution of MOZ to the transformation properties of MOZ-TIF2.

With respect to TIF2, our studies indicate that the CID is necessary and sufficient to activate the oncogenic potential of MOZ since a MOZ/CID mutant that retains only the CID from TIF2 shows full transforming properties in vitro and in vivo. This mutant fusion protein lacks numerous TIF2 domains required for DNA binding and protein heterodimerization (bHLH PAS

domain), nuclear receptor interaction (RID), and potential HAT activity (AD2) (Figure 1), indicating that these domains of TIF2 are also dispensable for transformation. We further demonstrate that MOZ-TIF2 associates with CBP through the TIF2 CID and that a MOZ-TIF2 LXXLL mutant abrogates transformation.

Our results have three potential implications for the mechanistic role of MOZ-TIF2 in mediating leukemic transformation. Firstly, MOZ-TIF2 promotes leukemogenesis through a dominant gain of MOZ function via direct transcriptional deregulation. In such a model, the C2HC zinc finger motif facilitates specific recognition of nucleosomal components positioned at transcriptional elements within the regulatory sequences of MOZ target genes. How the MOZ C2HC motif discriminates nucleosomes and/or DNA sequences in the context of MOZ target genes is currently unknown. The TIF2 moiety within MOZ-TIF2, no longer nuclear hormone responsive, may constitutively recruit CBP. Once recruited to MOZ target genes via the CID within TIF2, CBP could serve as an aberrant constitutive coactivator. For the related MOZ-CBP fusion protein, the CBP moiety is covalently coupled to MOZ and would therefore also result in constitutive coactivation of MOZ target genes. Thus, MOZ-TIF2 may mimic the MOZ/CBP fusion in the t(8;16) associated with AML M5 subtype (Borrow et al., 1996), and these two fusion proteins may share overlapping molecular targets that contribute a common pathway to leukemia pathogenesis.

CBP transcriptional coactivation requires either CBP HAT or the CBP-associated P/CAF HAT activity (Korzus et al., 1998). Thus, CBP-dependent acetylation of nucleosomes may enhance chromatin accessibility surrounding transcriptional elements within the regulatory sequences of MOZ target genes, indirectly facilitating the engagement of additional transcriptional complexes that aberrantly initiate and/or maintain MOZ target gene expression. In support of this model, the MOZ/CBP fusion associated with t(8;16) blocks IL-6-induced terminal differentiation of M1 cells in vitro via a HAT domain-dependent mechanism, suggesting that HAT activity of CBP may have an essential role in transformation of certain cell lines (Kitabayashi et al., 2001a). However, we currently cannot exclude the possibility that collaboration between MOZ-TIF2 and CBP occurs via a HAT-independent mechanism in which CBP acts as a bridging molecule to recruit other transcription factors to MOZ target genes whereby transcriptional activation takes place in a chromatin environment that is already competent for transcription.

Secondly, histones are not the exclusive in vivo substrates for CBP-associated acetyltransferase activity. CBP also exhibits factor acetyltransferase (FAT) activity to modulate the function of a growing number of transcription factors including p53 (Gu and Roeder, 1997), hematopoietic cell-specific factor GATA-1 (Boyes et al., 1998), and EKLF (Zhang and Bieker, 1998; Hung et al., 1999). Therefore, aberrant acetylation of these of other as yet undefined transcriptional factors by the MOZ-TIF2-CBP complex may contribute to leukemogenesis.

Thirdly, the interaction of CBP with MOZ-TIF2 may result in *trans*-dominant inhibition of CBP tumor suppressor function. CBP displays tumor suppressor properties in heterozygous mice (Kung et al., 2000) as well as humans with Rubinstein-Taybi syndrome (Petrij et al., 1995), leading to an increased propensity for hematologic malignancies in both settings. However, we do not favor this possibility in MOZ-TIF2-induced leukemias. If the function of the MOZ-TIF2 fusion were simply to bind and sequester CBP, resulting in physiologic loss of CBP function, then it could be predicted that the MOZ nucleosomal recognition motif would not be required for transformation. However, MOZ-TIF2 with a point mutation in the C2HC nucleosome recognition motif is not transforming. Our data are thus more consistent with the hypothesis that MOZ-TIF2 results in MOZ gain of function through recruitment of CBP to MOZ targets and suggest the novel finding that CBP contributes an oncogenic rather than tumor-suppressive function to myeloid transformation by MOZ-TIF2. These studies provide insights into the molecular mechanism of transformation mediated by MOZ-TIF2 and provide tools for understanding the mechanism of leukemias mediated by HAT domain fusion proteins.

Experimental procedures

Plasmid and mutant construction

To construct the expression vector *pcDNA3-MOZ-TIF2(I)*, the breakpoint region was PCR amplified from patient cDNA (Carapeti et al., 1998) and ligated to 5′ *MOZ* fragment obtained from *pBS-MOZ* (kindly provided by J. Borrow) and 3′ *TIF2* fragment obtained from *pSG5-TIF2* (kindly provided by H. Gronemeyer) by two step ligation. *pcDNA3-MOZ-TIF2(II)*, *MOZ/delCID*, and the *MOZ-TIF2-LXXLL* mutant were kindly provided by K. Blanchard. *pcDNA3-delPHD/TIF2*, *delHAT/TIF2*, *MOZ-TIF2-C543G* (C2HC finger mutant), and the *MOZ-TIF2-G657E* (acetyl-CoA binding site mutant) were constructed using site-directed mutagenesis (ExSite™ PCR-Based®; Stratagene, La Jolla, California) of *pcDNA3-MOZ-TIF2(II)* according to the manufacturer's instructions. *pcDNA-MOZ/CID* was constructed by introducing a *MOZ/CID* fragment from *MSCV2.2 GFP-MOZ/CID* (as below) digested with EcoRI to the EcoRI site of pcDNA.

The full-length cDNAs were subcloned from pcDNA to *MSCV-EB* neo at the EcoRI site or XhoI site, or *MSCV2.2* GFP into the EcoRI site or XhoI-EcoRI sites. The *MSCV-MOZ/CID* constructs were generated by digesting *MSCV-MOZ-TIF2* constructs followed by a self-ligation step that resulted in an out-of-frame fusion 3′ of the TIF2 CID.

For analysis of protein expression of pcDNA or MSCV constructs, Kozak and Flag sequences (GCCACC and ATGGATTACAAGGATGACGACGAT AAG) were introduced into the 5′ portion of the cDNA by site-directed mutagenesis and used for Western blotting.

MOZ cDNA was cloned in-frame into the vector pMAL-c2x (New England BioLabs, Beverly, Massachusetts) downstream from the maltose binding protein (MBP) purification tag to generate the construct pMAL-*MOZ*. The constructs pMAL-*MOZ-C543G* and pMAL-*MOZ-G657E* were derived from the wild-type construct using site-directed mutagenesis (QuikChange®; Stratagene).

pGEX-4T1-CBP, which expressed a glutathione S-transferase (GST) fusion protein containing the p160 family binding domain of murine CBP, was generated by introducing *CBP* fragment (aa2040-2200) made by PCR into BamHI-EcoRI sites.

All constructs were confirmed by DNA sequencing.

Myeloid immortalization assay

Transduction of murine bone marrow (BM) cells was performed essentially as described previously (DiMartino, et al., 2000). Briefly, 4-week-old C57B/6 mice were injected with 5-FU (150 mg/kg) by tail vein, and bone marrow was harvested from both femurs after 5 days. Transient retroviral supernatants were produced by transfecting NX cells with *MSCV* vectors as described previously (Pear et al., 1993). Bone marrow cells were infected with recombinant virus by centrifugation at 2500 × g for 2 hr at 32°C. Transduced cells were plated in 0.9% methylcellulose (Stem Cell Technologies, Vancouver, BC, Canada) supplemented with 20 ng/ml stem cell factor (SCF) and 10 ng/ml each of interleukin-3 (IL-3) and IL-6 (R&D Systems, Minneapolis, Minnesota) in the presence or absence of G418 (1 mg/ml). After 7 to 10 days, colonies were counted and retroviral transduction efficiency was calculated for each construct as the ratio of G418-resistant (G418R) colonies to unselected colonies. Single cell suspensions were made from pooled G418R colonies, and 10^4 cells were plated in secondary methylcellulose cultures without G418.

Murine bone marrow transplant assay

Retroviral supernatant were generated by transient cotransfection of 293T cells with the *MSCV-IRES-EGFP* constructs and packaging plasmid (Ecopac) using Superfect (Qiagen, Valencia) according to the manufacturer's instructions. Supernatants were collected 48 hr posttransfection and filtered (0.45 μm). Viral titers were estimated by transduction of Ba/F3 cells in the presence of Polybrene (10 mg/ml) as described previously (Liu et al., 2000). Eight days prior to each BMT procedure, 4- to 6-week-old male BALB/c mice (from Taconic, Germantown, New York) were pretreated with 150 mg of 5-fluorouracil (5-FU; Sigma) per kg body weight, administered intraperitoneally. Two days prior, bone marrow was harvested from these donor mice by flushing femurs and tibias and red blood cells were lysed. Bone marrow cells were then resuspended in RPMI/10% FBS supplemented with 6 ng/ml recombinant mouse IL-3 (Genzyme, Cambridge, Massachusetts), 100 ng/ml recombinant mouse stem cell factor (Genzyme), and 10 ng/ml recombinant mouse IL-6 (PeproTech, Rocky Hill, New Jersey) and cultured overnight at 37°C. Cells were transduced by two rounds of spin infection at 24 hr and 48 hr after harvesting. Centrifugation of 1 ml viral supernatant and 4×10^6 cells in 3 ml transplant media containing 5 μg/ml Polybrene and 7.5 mM HEPES buffer was carried out for 90 min at 1800 g. Cells were washed in PBS, resuspended in Hanks balanced salt solution (Life Technologies), and injected ($1–2 \times 10^6$ cells/0.5 ml) into the lateral tail vein of lethally irradiated ($2 \times$ 450 cGy) female syngeneic recipient mice. Mice were housed in microisolator cages with autoclaved chow and acidified water.

Southern blot analysis

Genomic DNA was isolated from tissues using tissue lysis buffer (100 nM Tris-HCl, 5 mM EDTA, 0.2% SDS, 200 mM NaCl, 100 μg/ml proteinase K). Ten micrograms of each DNA was digested with either NheI (cleaves twice, at the LTR's in the provirus) or EcoRI (cleaves once or twice at the upstream of EGFP part of retrovirus) and transferred to Hybond N^+ nylon membranes (Amersham, Arlington Heights, Illinois). Provirus was detected using an EGFP probe.

Western blot analysis

The 293T cells transiently transfected with *MSCV* constructs were washed three times in PBS and lysed in 50 mM HEPES (pH 7.5), 0.2 mM EDTA, 0.5% NP40, 10 μM NaF, 250 mM NaCl. Equal volume of cell lysate was separated on a 5% gel and Western analysis was performed as described previously (Kelly et al., 2002) using 1 μg/ml anti-Flag M2 antibody (Upstate, New York) as the primary antibody, followed by horseradish peroxidase-conjugated secondary antibody (Amersham Life Science) and visualization by enhanced chemoluminescence (Amersham Life Science).

Histopathology

Murine tissues were fixed for 24 hr in 10% neutral buffered formalin and embedded in paraffin. Femurs were subjected to an additional decalcification step in RDO (Apex Engineering Products, Planfield, Illinois) for 0.5–1 hr prior to processing. Sections (4 μm) were deparaffinized and stained with hematoxylin-eosin (HE). Smears of peripheral blood cells and touch preparations of lymph node were stained with Wright-Giemsa (WG).

Flow cytometry

Single cell suspensions were processed for flow cytometry as described previously (Schwaller et al., 1998; Tomasson et al., 2000). To block nonspecific Fc receptor-mediated binding, the cells were preincubated for 20 min at 4°C with supernatant from the 2.4G2 hybridoma cell line (American Type Culture Collection, Rockville, Maryland) producing antibodies recognizing CD16 and CD32. Cells were stained for 20 min on ice with monoclonal antibodies conjugated with phycoerythrin (PE), allophycocyanin (APC), or biotin. The antibodies used were PE conjugates of anti-Mac-1 (CD11b), anti-Thy-1.2, anti-c-kit, and APC-conjugated anti-Gr-1 and biotinylated anti-CD19, anti-CD34 (all antibodies purchased from PharMingen, San Diego, California). The binding of the biotinylated primary antibodies was detected using APC-conjugated streptavidin (Caltag, South San Francisco, California). Cells were washed once in FACS staining buffer (PBS/1%FBS/0.1% sodium azide) and multicolor flow cytometric analysis was carried out with a FACS-Calibur (Becton-Dickinson). A minimum of 10,000 events was acquired and the data were analyzed using CellQuest v3.1 software (Becton-Dickinson Immunocytometry Systems, San Jose, California). The results are presented as dot plots of cells that were gated on the basis of forward and side scatter. In some experiments, gating for EGFP expression was also done.

HAT assays

Bacterially expressed MBP and MBP-MOZ proteins were purified on amylose beads according to the manufacturer's instructions. The concentrations of purified MBP proteins were determined spectrophotometrically by comparison to a standard curve prepared using bovine serum albumin. The purity and integrity of eluted MBP and MBP-MOZ proteins was assessed by SDS-PAGE. Purified MBP proteins were used in histone acetyltransferase assays.

HAT activity was determined by measuring the incorporation of [^{3}H]acetyl CoA (Amersham Biosciences) into calf thymus histones (Type IIA; Sigma Chemical, St. Louis, Missouri) in liquid assays according to published methods (Mizzen et al., 1999). Ten micrograms of each protein sample was assessed for HAT activity in a 50 μl reaction buffer containing 5 μg calf thymus histones. Incubations were performed for 20 min at 30°C. The incorporation of ^{3}H-acetate into free histone substrates was quantitated by P81 filter binding and liquid scintillation. Triplicate 15 μl aliquots of each reaction mix were processed in parallel. The assay was repeated to confirm the reproducibility of the findings.

GST pulldown assays with [35^S]methionine-labeled proteins

Bacterial lysates containing GST or GST fusion proteins were incubated at 4°C for 2 hr with Glutathione-Sepharose beads (Pharmacia). 35S-labeled samples produced from pcDNA constructs as a template by in vitro translation using the TNT T7-coupled reticulocyte lysate system (Promega) were added to 500 ml of binding buffer (20 mM HEPES [pH 7.8], 75 mM KCl, 0.1 mM EDTA, 2.5 mM MgCl2, 1% skim milk,1 mM DTT, 0.05% NP-40) containing the preabsorbed beads and then the mixture was incubated at 4°C for 2 hr. Bound proteins were recovered in SDS sample buffer and analyzed by SDS-PAGE and autoradiography.

Acknowledgments

We gratefully acknowledge technical and administrative assistance from Alexis Bywater, and discussions with members of the Glass, Cleary, and Gilliland labs. This work was supported in part by NIH NCI CA66996, DK50654 (D.G.G.), CA55029 (M.L.C.), the Leukemia and Lymphoma Society (K.D. and D.G.G.), and the Mochida Memorial Foundation (K.D.). K.D. is a Research Associate and D.G.G. is an Associate Investigator of the Howard Hughes Medical Institute.

Received: November 12, 2002
Revised: January 30, 2003

References

Akhtar, A., and Becker, P.B. (2000). Activation of transcription through histone H4 acetylation by MOF, an acetyltransferase essential for dosage compensation in Drosophila. Mol. Cell *5*, 367–375.

Akhtar, A., and Becker, P.B. (2001). The histone H4 acetyltransferase MOF uses a C2HC zinc finger for substrate recognition. EMBO Rep. *2*, 113–118.

Ayton, P.M., and Cleary, M.L. (2001). Molecular mechanisms of leukemogenesis mediated by MLL fusion proteins. Oncogene *20*, 5695–5707.

Billio, A., Steer, E.J., Pianezze, G., Svaldi, M., Casin, M., Amato, B., Coser, P., and Cross, N.C. (2002). A further case of acute myeloid leukaemia with inv(8)(p11q13) and MOZ- TIF2 fusion. Haematologica *87*, ECR15.

Borrow, J., Stanton, V.P., Jr., Andresen, J.M., Becher, R., Behm, F.G., Chaganti, R.S., Civin, C.I., Disteche, C., Dube, I., Frischauf, A.M., et al. (1996). The translocation t(8;16)(p11;p13) of acute myeloid leukaemia fuses a putative acetyltransferase to the CREB-binding protein. Nat. Genet. *14*, 33–41.

Boyes, J., Byfield, P., Nakatani, Y., and Ogryzko, V. (1998). Regulation of activity of the transcription factor GATA-1 by acetylation. Nature *396*, 594–598.

Carapeti, M., Aguiar, R.C., Goldman, J.M., and Cross, N.C. (1998). A novel

fusion between MOZ and the nuclear receptor coactivator TIF2 in acute myeloid leukemia. Blood *91*, 3127–3133.

Chaffanet, M., Gressin, L., Preudhomme, C., Soenen-Cornu, V., Birnbaum, D., and Pebusque, M.J. (2000). MOZ is fused to p300 in an acute monocytic leukemia with t(8;22). Genes Chromosomes Cancer *28*, 138–144.

Chakraborty, S., Senyuk, V., and Nucifora, G. (2001). Genetic lesions and perturbation of chromatin architecture: a road to cell transormation. J. Cell. Biochem. *8*, 310–325.

Champagne, N., Pelletier, N., and Yang, X.J. (2001). The monocytic leukemia zinc finger protein MOZ is a histone acetyltransferase. Oncogene *20*, 404–409.

Demarest, S.J., Martinez-Yamout, M., Chung, J., Chen, H., Xu, W., Dyson, H.J., Evans, R.M., and Wright, P.E. (2002). Mutual synergistic folding in recruitment of CBP/p300 by p160 nuclear receptor coactivators. Nature *415*, 549–553.

Ding, X.F., Anderson, C.M., Ma, H., Hong, H., Uht, R.M., Kushner, P.J., and Stallcup, M.R. (1998). Nuclear receptor-binding sites of coactivators glucocorticoid receptor interacting protein 1 (GRIP1) and steroid receptor coactivator 1 (SRC-1): multiple motifs with different binding specificities. Mol. Endocrinol. *12*, 302–313.

DiMartino, J.F., Miller, T., Ayton, P.M., Landewe, T., Hess, J.L., Cleary, M.L., and Shilatifard, A. (2000). A carboxy-terminal domain of ELL is required and sufficient for immortalization of myeloid progenitors by MLL-ELL. Blood *96*, 3887–3893.

Glass, C.K., Rose, D.W., and Rosenfeld, M.G. (1997). Nuclear receptor coactivators. Curr. Opin. Cell Biol. *9*, 222–232.

Grant, P.A., and Berger, S.L. (1999). Histone acetyltransferase complexes. Semin. Cell Dev. Biol. *10*, 169–177.

Gu, W., and Roeder, R.G. (1997). Activation of p53 sequence-specific DNA binding by acetylation of the p53 C-terminal domain. Cell *90*, 595–606.

Heery, D.M., Kalkhoven, E., Hoare, S., and Parker, M.G. (1997). A signature motif in transcriptional co-activators mediates binding to nuclear receptors. Nature *387*, 733–736.

Horwitz, K.B., Jackson, T.A., Bain, D.L., Richer, J.K., Takimoto, G.S., and Tung, L. (1996). Nuclear receptor coactivators and corepressors. Mol. Endocrinol. *10*, 1167–1177.

Hung, H.L., Lau, J., Kim, A.Y., Weiss, M.J., and Blobel, G.A. (1999). CREB-binding protein acetylates hematopoietic transcription factor GATA-1 at functionally important sites. Mol. Cell. Biol. *19*, 3496–3505.

Ida, K., Kitabayashi, I., Taki, T., Taniwaki, M., Noro, K., Yamamoto, M., Ohki, M., and Hayashi, Y. (1997). Adenoviral E1A-associated protein p300 is involved in acute myeloid leukemia with t(11;22)(q23;q13). Blood *90*, 4699–4704.

Kelly, L.M., Liu, Q., Kutok, J.L., Williams, I.R., Boulton, C.L., and Gilliland, D.G. (2002). FLT3 internal tandem duplication mutations associated with human acute myeloid leukemias induce myeloproliferative disease in a murine bone marrow transplant model. Blood *99*, 310–318.

Kitabayashi, I., Aikawa, Y., Nguyen, L.A., Yokoyama, A., and Ohki, M. (2001a). Activation of AML1-mediated transcription by MOZ and inhibition by the MOZ-CBP fusion protein. EMBO J. *20*, 7184–7196.

Kitabayashi, I., Aikawa, Y., Yokoyama, A., Hosoda, F., Nagai, M., Kakazu, N., Abe, T., and Ohki, M. (2001b). Fusion of MOZ and p300 histone acetyltransferases in acute monocytic leukemia with a t(8;22)(p11;q13) chromosome translocation. Leukemia *15*, 89–94.

Klein-Hitpass, L., Tsai, S.Y., Weigel, N.L., Allan, G.F., Riley, D., Rodriguez, R., Schrader, W.T., Tsai, M.J., and O'Malley, B.W. (1990). The progesterone receptor stimulates cell-free transcription by enhancing the formation of a stable preinitiation complex. Cell *60*, 247–257.

Korzus, E., Torchia, J., Rose, D.W., Xu, L., Kurokawa, R., McInerney, E.M., Mullen, T.M., Glass, C.K., and Rosenfeld, M.G. (1998). Transcription factor-specific requirements for coactivators and their acetyltransferase functions. Science *279*, 703–707.

Kung, A.L., Rebel, V.I., Bronson, R.T., Ch'ng, L.E., Sieff, C.A., Livingston, D.M., and Yao, T.P. (2000). Gene dose-dependent control of hematopoiesis and hematologic tumor suppression by CBP. Genes Dev. *14*, 272–277.

Lavau, C., Szilvassy, S.J., Slany, R., and Cleary, M.L. (1997). Immortalization and leukemic transformation of a myelomonocytic precursor by retrovirally transduced HRX-ENL. EMBO J. *16*, 4226–4237.

Lavau, C., Du, C., Thirman, M., and Zeleznik-Le, N. (2000a). Chromatin-related properties of CBP fused to MLL generate a myelodysplastic-like syndrome that evolves into myeloid leukemia. EMBO J. *19*, 4655–4664.

Lavau, C., Luo, R.T., Du, C., and Thirman, M.J. (2000b). Retrovirus-mediated gene transfer of MLL-ELL transforms primary myeloid progenitors and causes acute myeloid leukemias in mice. Proc. Natl. Acad. Sci. USA *97*, 10984–10989.

Leo, C., and Chen, J.D. (2000). The SRC family of nuclear receptor coactivators. Gene *245*, 1–11.

Liang, J., Prouty, L., Williams, B.J., Dayton, M.A., and Blanchard, K.L. (1998). Acute mixed lineage leukemia with an inv(8)(p11q13) resulting in fusion of the genes for MOZ and TIF2. Blood *92*, 2118–2122.

Liu, Q., Schwaller, J., Kutok, J., Cain, D., Aster, J.C., Williams, I.R., and Gilliland, D.G. (2000). Signal transduction and transforming properties of the TEL-TRKC fusions associated with t(12;15)(p13;q25) in congenital fibrosarcoma and acute myelogenous leukemia. EMBO J. *19*, 1827–1838.

Mizzen, C.A., Brownell, J.E., Cook, R.G., and Allis, C.D. (1999). Histone acetyltransferases: preparation of substrates and assay procedures. Methods Enzymol. *304*, 675–696.

Panagopoulos, I., Fioretos, T., Isaksson, M., Samuelsson, U., Billstrom, R., Strombeck, B., Mitelman, F., and Johansson, B. (2001). Fusion of the MORF and CBP genes in acute myeloid leukemia with the t(10;16)(q22;p13). Hum. Mol. Genet. *10*, 395–404.

Pear, W.S., Nolan, G.P., Scott, M.L., and Baltimore, D. (1993). Production of high-titer helper-free retroviruses by transient transfection. Proc. Natl. Acad. Sci. USA *90*, 8392–8396.

Pelletier, N., Champagne, N., Stifani, S., and Yang, X.J. (2002). MOZ and MORF histone acetyltransferases interact with the Runt-domain transcription factor Runx2. Oncogene *21*, 2729–2740.

Petrij, F., Giles, R.H., Dauwerse, H.G., Saris, J.J., Hennekam, R.C., Masuno, M., Tommerup, N., van Ommen, G.J., Goodman, R.H., Peters, D.J., et al. (1995). Rubinstein-Taybi syndrome caused by mutations in the transcriptional co-activator CBP. Nature *376*, 348–351.

Satake, N., Ishida, Y., Otoh, Y., Hinohara, S., Kobayashi, H., Sakashita, A., Maseki, N., and Kaneko, Y. (1997). Novel MLL-CBP fusion transcript in therapy-related chronic myelomonocytic leukemia with a t(11;16)(q23;p13) chromosome translocation. Genes Chromosomes Cancer *20*, 60–63.

Schwaller, J., Frantsve, J., Aster, J., Williams, I.R., Tomasson, M.H., Ross, T.S., Peeters, P., Van Rompaey, L., Van Etten, R.A., Ilaria, R., Jr., et al. (1998). Transformation of hematopoietic cell lines to growth-factor independence and induction of a fatal myelo- and lymphoproliferative disease in mice by retrovirally transduced TEL/JAK2 fusion genes. EMBO J. *17*, 5321–5333.

Slany, R.K., Lavau, C., and Cleary, M.L. (1998). The oncogenic capacity of HRX-ENL requires the transcriptional transactivation activity of ENL and the DNA binding motifs of HRX. Mol. Cell. Biol. *18*, 122–129.

Sobulo, O.M., Borrow, J., Tomek, R., Reshmi, S., Harden, A., Schlegelberger, B., Housman, D., Doggett, N.A., Rowley, J.D., and Zeleznik-Le, N.J. (1997). MLL is fused to CBP, a histone acetyltransferase, in therapy-related acute myeloid leukemia with a t(11;16)(q23;p13.3). Proc. Natl. Acad. Sci. USA *94*, 8732–8737.

Sterner, D.E., and Berger, S.L. (2000). Acetylation of histones and transcription-related factors. Microbiol. Mol. Biol. Rev. *64*, 435–459.

Takechi, S., and Nakayama, T. (1999). Sas3 is a histone acetyltransferase and requires a zinc finger motif. Biochem. Biophys. Res. Commun. *266*, 405–410.

Taki, T., Sako, M., Tsuchida, M., and Hayashi, Y. (1997). The t(11;16)(q23;p13) translocation in myelodysplastic syndrome fuses the MLL gene to the CBP gene. Blood *89*, 3945–3950.

Tomasson, M.H., Sternberg, D.W., Williams, I.R., Carroll, M., Cain, D., Aster, J.C., Ilaria, R.L., Jr., Van Etten, R.A., and Gilliland, D.G. (2000). Fatal myeloproliferation, induced in mice by TEL/PDGFbetaR expression, depends on PDGFbetaR tyrosines 579/581. J. Clin. Invest. *105*, 423–432.

Torchia, J., Rose, D.W., Inostroza, J., Kamei, Y., Westin, S., Glass, C.K., and Rosenfeld, M.G. (1997). The transcriptional co-activator p/CIP binds CBP and mediates nuclear-receptor function. Nature *387*, 677–684.

Voegel, J.J., Heine, M.J., Tini, M., Vivat, V., Chambon, P., and Gronemeyer, H. (1998). The coactivator TIF2 contains three nuclear receptor-binding motifs and mediates transactivation through CBP binding-dependent and -independent pathways. EMBO J. *17*, 507–519.

Zhang, W., and Bieker, J.J. (1998). Acetylation and modulation of erythroid Kruppel-like factor (EKLF) activity by interaction with histone acetyltransferases. Proc. Natl. Acad. Sci. USA *95*, 9855–9860.